Optical and Photocatalytic Properties of $BiVO_4$ Particles Derived via Rapid Synthesis Sonochemical Process

Thanaphon Kansaard[1,*], Chatpong Bangbai[2] and Chakkaphan Wattanawikkam[3]

[1] *College of Materials Innovation and Technology, King Mongkut's Institute of Technology Ladkrabang, Ladkrabang, Bangkok, 10520, Thailand*

[2] *Department of Science and Mathematics, Faculty of Science and Health Technology, Kalasin University, Kalasin, 46000, Thailand*

[3] *Faculty of Science and Technology, Rajamangala University of Technology Thanyaburi, Pathumthani, 12110, Thailand*

Received: 21 November 2023, Revised: 26 December 2023, Accepted: 27 December 2023

Abstract

Currently, environmental pollution is very critical to human health and nature. For solving these problems, photocatalytic degradation by metal oxide materials is among effective organic compound decomposition methods. $BiVO_4$ is an attractive material due to light activation under visible irradiation. This work focuses on the rapid synthesis of $BiVO_4$ via sonochemical process within 30 min. Ultrasonic irradiation time determined as a crucial parameter of particle formation was designated in range of 0-30 min. The crystalline structure of superior condition shows the pure monoclinic phase of $BiVO_4$with optical band gap value 2.5 eV by Kubelka-Munk function calculation. The Raman scattering result confirmed the bonding of $BiVO_4$ and XANES result exhibited the confirmation of Bi^{3+} and V^{5+} formation in $BiVO_4$ material. The superior photocatalytic activity under revealed in BV-30 sample with decomposition rate 0.0032 min^{-1} (R^2 = 0.98*)* under visible light exposure. The lowest the photoluminescence spectrum confirmed the minor recombination of electron-hole from photogeneration. This integrated analysis underscores the favorable structural, optical, and chemical properties of the $BiVO_4$ material synthesized with a 30 minute of ultrasonic irradiation time, making it a promising candidate for efficient photocatalysis under visible light conditions.

Keywords: Sonochemical process, Bismuth vanadate, Photocatalyst

1. Introduction

Environmental pollution problems such as wastewater, toxic gas and organic volatile are among critical issues to be concerned with and request an attempt to eradicate. For solving these problems, photocatalytic degradation by metal oxide materials such as ZnO, TiO_2, Bi_2WO_6 and $BiVO_4$ has been considered as one of effective decomposition methods [1], [2]. Among metal oxide photocatalysts, $BiVO_4$ one of orthovanadate MVO_4 based materials is recognized as an alternative photocatalyst material owing to considerable advantages including good chemical stability, low toxicity, visible-light active ability, and ease of synthesis by various methods such as co-precipitation, hydrothermal or solvothermal and solid-state reaction method. Generally, $BiVO_4$ materials can be found in two crystal structures of Clinobisvanite monoclinic and scheelite tetragonal. Both crystal structures can be formed under different environments such as high temperature or high pressure [3]. The previous work reported that high temperature about 200°C for hydrothermal or calcination temperature about 800°C for another method was required to

Corresponding Author : tkansaard@gmail.com

achieve the formation of this material [4], [5]. Therefore, one-step synthesis or facile process is of interest and still is required for this material. The sonochemical process stands out as an excellent candidate for the preparation of metal-oxide-based materials. This is attributed to its non-complex system, absence of external treatments, and the utilization of very short reaction times. Sonochemical processes requiring only intense ultrasonic energy for chemical reaction and nucleation is considered as facile one-step synthesis method without other treatment [6], [7]. In this work, rapid sonochemical process was employed to synthesize $BiVO_4$ nanoparticles, and the influence of short ultrasonic irradiation times ranging from 0 to 30 minutes on the structural, optical, and photocatalytic performance of the synthesized powders was investigated. The photocatalytic performance under visible light irradiation of the prepared photocatalyst was evaluated by the decomposition of Rhodamine B dye (RhB) as aqueous organic compound model.

2. Experimental

2.1 Materials

Bismuth nitrate pentahydrate ($Bi(NO_3)_3.5H_2O$) designated as bismuth source was purchased from Ajax finechem., Ltd while Ammonium metavanadate (NH_4VO_3) used as vanadium source was supplied by Sigma Aldrich company.

2.2 Synthesis of $BiVO_4$

As-prepared Bismuth vanadate samples were synthesized by sonochemical method with different ultrasonic irradiation times ranging from 0-30 min. At first, 0.1 mol bismuth nitrate pentahydrate assigned as bismuth source was dissolved in 100 ml deionized water (DI-water) then stirred at room temperature while ammonium meta vanadate was separately dissolved in DI-water to attain same concentration. Both precursors were mixed homogeneously under continuous stirring and the pH value of mixed solution was adjusted to reach pH=7 by using ammonium hydroxide and keep continuous stirring for 15 min. After the mixed solution was transferred to sonochemical chamber, 750 W ultrasonic sound operated at 20 kHz was directly supplied to the chamber with various irradiation times of 4, 8, 12, 16, 20, and 30 min to obtain the yellowish colloidal solution. The colloid of each condition was washed with DI water followed by filtration and drying process at 100°C overnight until dried specimen powders was achieved.

2.3 Characterizations

Crucial properties of the prepared samples were extensively investigated. Their crystalline structure was characterized by X-Ray diffraction technique using Cu-K_α as an X-ray source while relevant chemical bonding and optical properties were investigated by Raman scattering technique (Thermo Scientific DRX SmartRaman) and diffuse reflectance spectroscopy (LAMDA 850+, PerkinElmer), respectively. Photoluminescence spectra of all samples were carried using fluorescence spectrophotometer (FluoroMaxplus, Horiba Scientific) with excitation wavelength of 352 nm. X-ray absorption spectroscopy (XAS) was employed to further study the local structure. V K-edge and Bi L_3-edge of X-ray absorption near-edge structure (XANES) measurement were conducted at beamline-8 (BL8) of Synchrotron Light Research Institute (SLRI), Nakhon Rachasima, Thailand. The BL8 is a bending magnet beamline which has energy of 1.2 GeV with 80-120 mA for beam current. The collected data were performed in transmission mode for V K-edge (5,465 eV) and fluorescent mode for Bi L_3-edge (1,3419 eV) by Ge220 double crystal monochromator.

2.4 Photocatalytic testing

Photocatalytic performance of the prepared materials was evaluated by mean of the decomposition of Rhodamine B (RhB) organic dye under visible light irradiation. firstly, 100 mL of [RhB]10 μM for organic dye solution was prepared to be used as starting solution. 0.5 g prepared powder of each prepared condition was loaded to the organic dye solution and stirred under dark condition to attain adsorption/desorption equilibrium for 30 min then 5 ml of test solution was kept for the first reference. Photocatalytic performance testing of each sample was operated under visible light irradiation (6W PHILIPS cool daylight LED stripe) for 120 min. During photocatalytic testing, 5 ml of the reaction solution was collected every 10 min. The concentration of degraded RhB solution was evaluated by means of its absorbance using UV-Visible spectrophotometer. The degradation feature of RhB solution was evaluated following equation: $D = A_t/A_0$, where A_0 is the absorbance of initial RhB and A_t is the absorption of decomposed RhB at designated irradiation time *(t)*.

3. Results and discussion

3.1 Crystalline structure

The crystalline structures of all $BiVO_4$ specimen (BV-X when X represents the ultrasonic irradiation time) are shown in Fig. 1. The XRD diffractograms of all samples exhibit the majority phase of $BiVO_4$ monoclinic phase indicating at the positions $2\theta = 18.9^o$, 28.9^o, 30.5^o, 34.5^o, 35.2^o, 39.7^o, 42.3^o, 45.8^o, 46.7^o, 47.2^o, 50.3^o, $53.2°$ and $58.5°$ corresponding to planes (011), (112), (004), (200), (020), (211), (105), (-123), (204), (024), (220), (116) and (132), respectively [JCPDS No. 01-083-1669]. Meanwhile, the minority phase at $2\theta = 24.4°$ belonging to $BiVO_4$ tetragonal structure can be observed for BV-0 to BV-12 samples due to the simple formation of tetragonal phase in general $BiVO_4$ crystal under normal environment [8]. In addition, no impurity phases of either Bi-based oxides or V-based oxides were detected. After the ultrasonic irradiation time was increased to 16 and 30 min the tetragonal structure was completely changed to monoclinic phase since the longer ultrasonic irradiation time could provide greater energy to the system that can initiate hot spot with ultrahigh temperature from the collapse of nanobubbles from acoustic cavitation phenomena in the sonochemical reactor. Higher temperature with higher thermal energy from cavitation effect in sonochemical process with certain irradiation time can consequently change the crystalline structure from tetragonal to monoclinic $BiVO_4$ [3], [9]. This result notifies that $BiVO_4$ particles can be synthesized via sonochemical process with shorten time and ultrasonic irradiation time is a crucial synthesis parameter for its phase transformation.

3.2 Chemical Bonding

The chemical bonding of $BiVO_4$ samples was investigated by Raman Scattering technique using LASER with wavelength of 532 nm as light source. The Raman scattering results of all samples are shown in Fig. 2. Raman shift at 813 cm^{-1} is ascribed to the vibration of V-O symmetric stretching of $BiVO_4$ monoclinic structure while couple peaks located at 373 and 332 cm^{-1} are typically associated to the symmetric and asymmetric bending mode of VO_4 tetrahedral structure, respectively. The lower peaks positioned at 197 and 118 cm^{-1} are attributed to the external mode of $BiVO_4$ photocatalyst material [10], [11]. The broad peak at 373-332 cm^{-1} and slightly shift of main peak around 800 cm^{-1} in the samples synthesized was obtained due to the mixed phases between of monoclinic and tetragonal structure splitting to double peaks for symmetric and asymmetric of VO_4 and V-O bonding length formation complex in BV-30 sample for pure monoclinic structure as shown in previous XRD result. The tetragonal phase could play a role to crystal distortion

in monoclinic structure in the $BiVO_4$ sample [3].

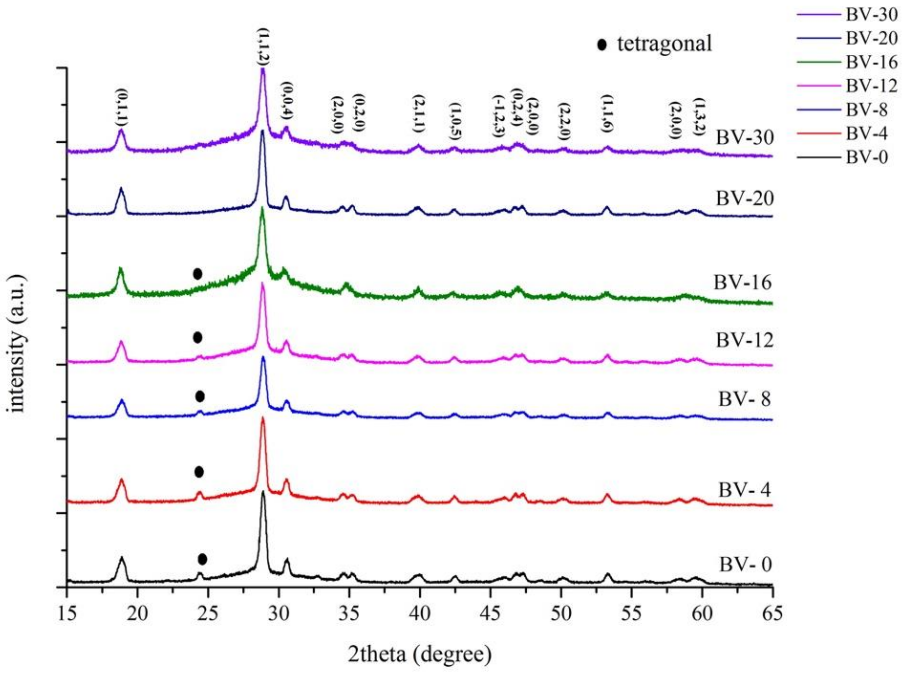

Fig. 1. X-ray diffractogram of $BiVO_4$ powder prepared by sonochemical process at different ultrasonic irradiation times

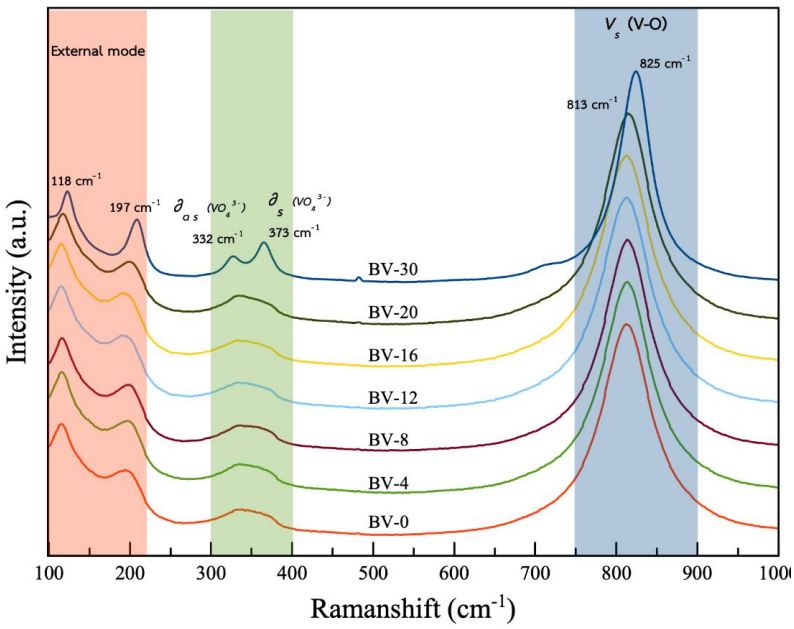

Fig. 2. Raman spectra of $BiVO_4$ samples prepared by sonochemical process with different ultrasonic irradiation times

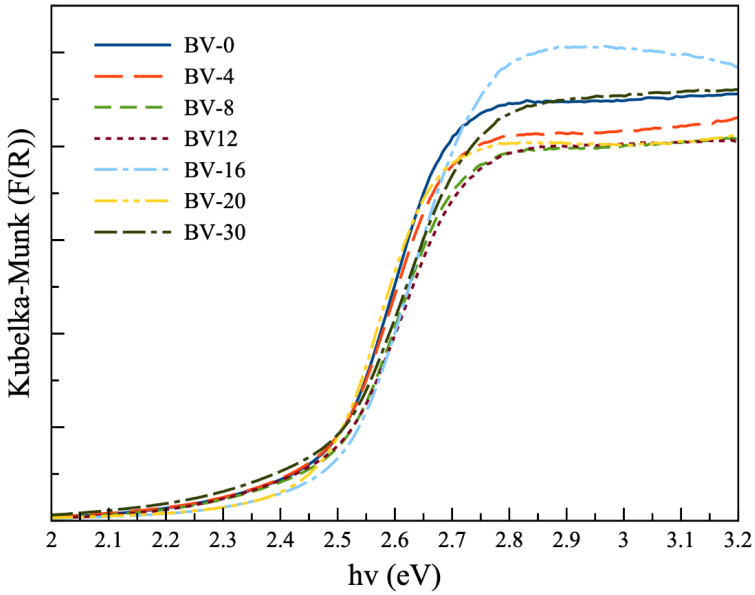

Fig. 3. Optical band gap calculation by Kubelka-Munk equation from diffuse reflectance spectra results of $BiVO_4$ samples prepared by sonochemical process with different ultrasonic irradiation times

3.3 Optical property

Optical behavior of $BiVO_4$ derived via sonochemical technique was investigated by diffuse reflectance spectrophotometer and its optical band gap was evaluated by Kubelka-Munk equation as shown in Fig. 3. The optical band gap energy of all specimens was calculated and evaluated to be approximately 2.5 eV with insignificant change in its band gap with respect to ultrasonic irradiation time. The calculated results are correlated to the energy band gap of monoclinic phase $BiVO_4$ photocatalyst material [12], [13]. The optical band gap energy of 2.5 eV suggesting that this material can be activated using visible light with corresponding wavelength shorter than 500 nm.

3.4 XANES analysis

The oxidation state of BV-30 sample was investigated by X-ray absorption near-edge structure (XANES) technique of V K-edge and Bi L_3-edge due to superior formation of monoclinic structure and exhibited the good photocatalytic performance observation. The XANES spectrum of Bi L_3-edge and V K-edge are shown in Fig 4. The XANES spectrum of Bi L_3-edge as shown in Fig. 4(a) includes Bi metal as reference spectra and BV-30 sample while Fig. 4(b) illustrates V K-edge spectra of V-foil, V_2O_5 for V^{5+} reference and BV-30. The XANES of Bi L_3-edge at absorption edge energy E_0 = 1,3418 eV is typical for Bi x-rays absorber. The main absorption peak of BV-30 sample for Bi L_3 edge is observed around 13,338 eV while the Bi metal shown the main absorption peak around 13,340 eV. The spectrum of BV-30 exhibits slight shift form Bi metal absorption spectrum due to the different neighboring atom of Bi atom in the crystal between Bi-metal and BV-30 sample [14]. Fig. 4(b) exhibits the difference in V K-edge absorption spectra of different specimens with various oxidation states of vanadium. V-foil (for V^0) shows an absorption edge at 5,465 eV while V_2O_5 for V^{5+} reference and BV-30 possess almost identical absorption edge at around 5,480 eV. This result suggests that the V ion in $BiVO_4$ monoclinic BV-30 must be in V^{5+} in the crystal corresponding to the VO_4 complex in $BiVO_4$ monoclinic

crystal structure [3], [15], [16].

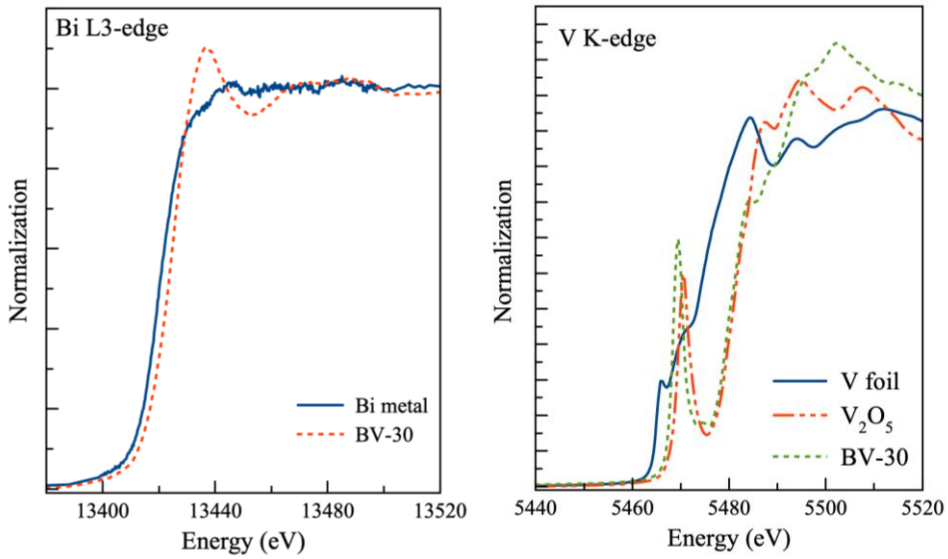

Fig. 4. XANES spectra of BV-30 sample investigated at Bi L3-edge and V K-edge comparing to standard references

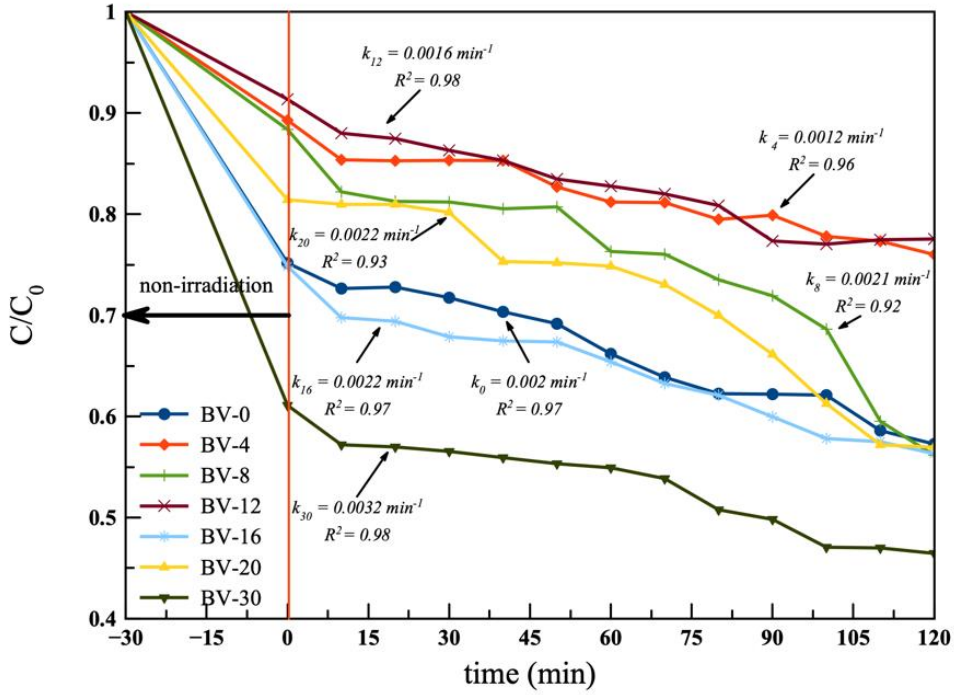

Fig. 5. Photodecomposition of Rhodamine-B organic dye under visible light irradiation using $BiVO_4$ samples prepared by sonochemical process with different ultrasonic irradiation times

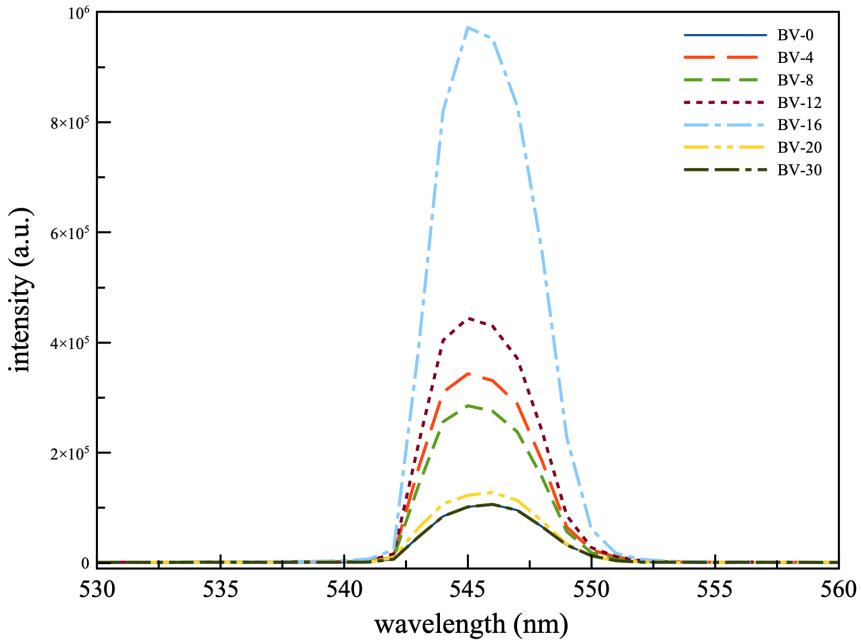

Fig. 6. Photoluminescence spectrum of $BiVO_4$ samples prepared by sonochemical process with different ultrasonic irradiation times

3.5 Photocatalyst testing

Photocatalytic activities under visible light exposure of $BiVO_4$ synthesized at different ultrasonic irradiation times were evaluated by mean of decomposition of organic compound using Rhodamine-B organic compound and corresponding results are depicted in Fig. 5. The activities were conducted for 120 min. After 30 min without irradiation (dark condition), the superior adsorption/desorption was obtained for BV-30 sample due to the surface absorption/desorption on the photocatalytic surface and the photodecomposition of RhB organic dye reached 50% after 120 min irradiation period. In the other hand, BV-4 and BV-12 sample exhibited inferiority in degradation of RhB with only 20% decomposition while approximately 40% degradation of RhB was achieved by BV-0, BV-8, BV16 and BV-20 photocatalyst samples. The highest decomposition activity of the BV-30 sample could be attributed to low recombination rate of active electron-hole pairs BV-30 photocatalyst generated during visible irradiation as supported by photoluminescence results in previous reports [17], [18]. Active electron-hole pairs are hence separated and mobilize to the photocatalyst surface where oxidation/reduction reactions with H_2O and O_2 leading to the generation of the hydroxyl radical and superoxide to become the active species for decomposition process of organic compound [19]-[22].

3.6 Photoluminescence

Photoluminescence (PL) spectra of $BiVO_4$ samples can be employed to evaluate the efficiency of photogenerated carriers correlated to the transfer, migration, and recombination process of photogenerated electron-hole pairs in the photocatalyst materials. Corresponding room temperature PL emission spectra under specific light excitation wavelength 352 nm of all sonochemically derived $BiVO_4$ are shown in Fig. 6. The broad emission spectra in the range of 540-550 nm were clearly observed in all $BiVO_4$ samples corresponding to intrinsic

luminescence between valence band and conduction band of hole and electron, respectively [23]. The strongest PL intensity was demonstrated in BV-16 while BV-30 sample exhibits the lowest emission intensity. This feature of low photoemission intensity of BV-30 suggests an enhancement in the separation of photogenerated electron-hole pairs behavior that can retard their recombination process. The high electron-hole pair separation during photogenerated process consequently results to high photodecomposition of RhB by BV-30 sample under visible light exposure. [17], [24] This superiority of this BV-30 sample could be attributed to the complete monoclinic phase $BiVO_4$ obtained at certain sonochemical reaction time.

4. Conclusion

This work was carried out to synthesize $BiVO_4$ photocatalyst material via rapid sonochemical process and ultrasonic irradiation was found to be an important synthesis parameter. The pure monoclinic crystal $BiVO_4$ was obtained after 30 min ultrasonic irradiation. The optical band gap of all $BiVO_4$ specimens was calculated and found to be 2.5 eV and the superior photocatalytic performance of as-prepared $BiVO_4$ was demonstrated in BV-30 sample with almost 50% decreasing of RhB, combined with surface absorption and degradation with $k = 0.0032$ min^{-1} ($R^2 = 0.98$) of RhB organic dye as organic compound model under visible light exposure due to the pure phase of monoclinic structure and lower electron-hole pair recombination suggested by its photoluminescence result.

Acknowledgment

This work was supported by Thailand Research Fund (TRF) through the Royal Golden Jubilee Ph.D. Program (grant no. PHD/0193/2556). Authors gratefully acknowledge to BL-8 at Synchrotron Light Research Institute (SLRI), Nakhon Rachasima, Thailand for XAS measurement and College of Materials Innovation and Technology (CMIT), King Mongkut's Institute of Technology Ladkrabang (KMITL) for facility support.

References

[1] Chala S, Wetchakun K, Phanichphant S, Inceesungvorn B, Wetchakun N, Enhanced visible-light-response photocatalytic degradation of methylene blue on Fe-loaded $BiVO_4$ photocatalyst. J. Alloy Compd. 2014;597:129-135.

[2] Tayyebi A, Soltani T, Lee B, Effect of pH on photocatalytic and photoelectrochemical (PEC) properties of monoclinic bismuth vanadate. J. Colloid Interface. Sci. 2019; 534: 37-46.

[3] Pellicer-Porres J, Vázquez-Socorro D, López-Moreno S, Muñoz A, Rodríguez-Hernández P, MMartínez-García D, *et. al.* Phase transition systematics in $BiVO_4$ by means of high-pressure-high-temperature Raman experiments. Phys. Rev. B. 2018; 98: 214109.

[4] Ravidhas C, Josephine A.J, Sudhagar P, Devadoss A, Terashima C, Nakata K, *et. al.* Facile synthesis of nanostructured monoclinic bismuth vanadate by a co-precipitation method: Structural, optical and photocatalytic properties. Mat. Sci. Semicon. Proc. 2015; 30:343-351.

[5] Ma J, Lin L, Chen Y, Facile solid-state synthesis for producing molybdenum and tungsten co-doped monoclinic $BiVO_4$ as the photocatalyst for photoelectrochemical water oxidation. Int. J. Hydrogen Energ. 2019;44:7905-14.

[6] Gotić M, Music S, Ivanda M, Šoufek M, Popović S, Synthesis and characterisation of bismuth (III) vanadate. J. Mol. Struct. 2005;744-747:535-40.

[7] Wattanawikkam C, Pecharapa W, Sonochemical synthesis, characterization, and photocatalytic activity of perovskite $ZnTiO_3$ nanopowders. IEEE. trans. Ultrason. Ferroelect. Freq. Control. 2016;63(10):1663-7.
[8] Fan H, Jiang T, Li H, Wang D, Wang L, Zhai J, He D, Wang P, Xie T, Effect of $BiVO_4$ crystalline phases on the photoinduced carriers behavior and photocatalytic activity. J. Phys. Chem. C. 2012;116: 2425-30.
[9] Liu W, Cao L, Su G, Liu H, Wang X, Zhang L, Ultrasound assisted synthesis of monoclinic structured spindle $BiVO_4$ particles with hollow structure and its photocatalytic property. Ultrason. Sonochem. 2010;17(4):669-74.
[10] Zhang A, Zhang J, Cui N, Tie X, An Y, Li L, Effects of pH on hydrothermal synthesis and characterization of visible-light-driven $BiVO_4$ photocatalyst. J. Mol.Catal. A-Chem. 2009;304(1-2):28-32.
[11] Yu J, Kudu A, Effects of structural variation on the photocatalytic performance of hydrothermally synthesized $BiVO_4$. Adv. Funct. Mater. 2016;16:2163-9.
[12] Zhou L, Wang W, Zhang L, Xu H, Zhu W, Single-crystalline $BiVO_4$ microtubes with square cross-sections: Microstructure, growth mechanism, and photocatalytic property. J. Phys. Chem. C. 2007;111:13659-64.
[13] Zhang X, Ai Z, Jia F, Zhang L, Fan X, Zou Z, Selective synthesis and visible-light photocatalytic activities of $BiVO_4$ with different crystalline phases. Mater. Chem. Phys. 2007; 103(1):162-7.
[14] Schwertfager N, Pandech N, Suewattana M, Thienprasert J.T, S. Limpijumnong, calculated XANES spectra of cation off-centering in $Bi(Mg_{0.5}Ti_{0.5})O_3$. Ferroelectrics. 2016;490:159-66.
[15] Trześniewski B, Digdaya I, Nagaki T, Ravishankar S, Heeraiz-Cardona I, Vermaas D, Longo A, Gimenez S, Smith W, Near-complete suppression of surface losses and total internal quantum efficiency in $BiVO_4$ photoanodes. Energy Environ. Sci. 2017;10:1517-29.
[16] Jovic V, Rettie AJ, Singh VR, Zhou J, Lamoureux B, Mullins CB, *et al.* A soft X-ray spectroscopic perspective of electron localization and transport in tungsten doped bismuth vanadate single crystals. Phys. Chem. Chem. Phys. 2016;18(46):31958-65.
[17] Li J, Cui M, Liu Z, Du J, Zhu Z, $BiVO_4$ hollow spheres with hierarchical microstructures and enhanced photocatalytic performance under visible-light illumination. Phys. Status Solidi A. 2013;210:1881-7.
[18] Lin X, Yu L, Yan L, Li H, Yan Y, Liu C, Zhai H, Visible light photocatalytic activity of $BiVO_4$ particles with different morphologies. Solid State Sci. 2014;32: 61-6.
[19] Jo W, Tayade R, Recent developments in photocatalytic dye degradation upon irradiation with energy-efficient light emitting diodes. Chin. J. Cat. 2014;35:1781-92.
[20] Yin W, Wang W, Zhou L, Sun S, Zhang L, CTAB-assisted synthesis of monoclinic $BiVO_4$ photocatalyst and its highly efficient degradation of organic dye under visible-light irradiation. J. Hazard. Mater. 2010;173(1-3):194-9.
[21] Jiang H, Liu J, Cheng K, Sun W, Lin J, Enhanced visible light photocatalysis of Bi_2O_3 upon fluorination. J. Phys. Chem. C. 2013;117(39):20029-36.
[22] Tokunaga S, Kato H, Kudo A, Selective preparation of monoclinic and tetragonal $BiVO_4$ with scheelite structure and their photocatalytic properties. Chem. Mater. 2001;13(12):4624-4628.
[23] Wu X, Zhou H, Gu S, Wang F, Liu J, Li W, In situ preparation of novel heterojunction BiOBr/$BiVO_4$ photocatalysts with enhanced visible light photocatalytic activity. RSC Adv. 2015;112(5):92769-77.
[24] Shan L, Liu Y, Er^{3+}, Yb^{3+} doping induced core–shell structured $BiVO_4$ and near-infrared photocatalytic properties. J. Mol.Catal. A-Chem. 2016;416:1-9.